A consistent and integrated network analysis framework for decoding interlinkages between sustainable development indicators at the global scale

Julien Ah-Pine[a,b], Elda Nasho Ah-Pine[c]

[a] *Université Clermont Auvergne, Clermont Auvergne INP, Mines Saint-Etienne, CNRS, LIMOS, F-63000 Clermont-Ferrand, France,*
[b] *Université Clermont Auvergne, CNRS, IRD, CERDI, F-63000 Clermont-Ferrand, France,*
[c] *Université Clermont Auvergne, Clermont School of Business, IAE Clermont Auvergne, CLERMA, F-63000 Clermont-Ferrand, France,*

Abstract

Achieving the United Nations Sustainable Development Goals (SDG) is crucial to addressing urgent global challenges such as poverty, inequality, environmental degradation, and climate change. The SDG aim to foster a more equitable, resilient, and sustainable future, yet their interdependent nature means that progress in one area often influences others, creating complex patterns of synergies and trade-offs. Navigating these systemic dynamics and development dilemmas requires robust, data-driven methods capable of capturing interactions at a granular level. This paper proposes a consistent and integrated framework for analyzing SDG indicators interlinkages at the global scale. We extend the Kendall correlation by incorporating population weighting and regional specificities, constructing a consistent signed weighted network of indicators. An optimal clustering method, aligned with eigenvector centrality, identifies structural groupings and systemic leverage points. We introduce an innovative visualization tool that reorganizes chord diagrams for greater interpretability and a bi-criteria Pareto front selection

to prioritize indicators based on influence and urgency. Applying the framework to the SDR 2024 dataset reveals critical synergies and trade-offs between SDG indicators, providing valuable insights for more effective policy design and highlighting the crucial roles of governance quality, environmental management, and urban infrastructure. Our approach provides a coherent toolset for policymakers seeking to design integrated, effective interventions that balance development and sustainability goals at global scale.
Keywords: Networks, SDG interlinkages, Kendall correlation, Graph clustering, Eigenvector centrality

---

1. Introduction

The 2030 Agenda for Sustainable Development, adopted by all United Nations (UN) member states in 2015, outlines 17 Sustainable Development Goals (SDG) and 169 targets aimed at balancing social, economic, and environmental progress (United Nations, 2015). Despite widespread commitment, progress remains insufficient, with less than 20% of SDG targets on track to be achieved by 2030 (Sachs et al., 2024). The slow and uneven trajectory demands not only accelerated action but also a shift toward coordinated, system-aware strategies.

Recent research increasingly emphasizes that siloed, sectoral interventions are inadequate to address the systemic complexity of sustainable development (Pradhan et al., 2024; Fuso Nerini et al., 2024; Kroll et al., 2019; Nilsson and Weitz, 2019; Pradhan et al., 2017). Consequently, there is a growing consensus on the necessity to map and quantify interlinkages among SDG variables to guide more coherent policy choices. Rigorous analysis of SDG interactions can reveal leverage points for maximizing positive spillovers

and preempt unintended cross-sectoral trade-offs (Pham-Truffert et al., 2020; Assubayeva and Marco, 2024).

This paper aims to contribute to the global governance of the SDG by proposing a framework for investigating interlinkages between indicators in an integrated and consistent manner, utilizing complementary analytical methods while accounting for regional specificities. Our approach offers a comprehensive way to understand the relationships between different SDG, with a particular focus on identifying potential synergies and trade-offs between indicators. By doing so, we aim to inform strategic priority-setting and foster more coherent solutions to accelerate progress toward the 2030 Agenda (Bennich et al., 2023). Our framework is characterized by a set of mutually coherent and interconnected technical features, including:

- A novel extension of Kendall correlation measure to assess the interlinkages between SDG indicators taking into account population sizes and regional dependencies.
- The application of an optimal clustering method to discover groups of indicators that are internally in positive relationships and mutually in negative relationships.
- The utilization of eigenvector centrality measure to detect which indicators are more important and influential in the SDG indicators network.
- The integration of the preceding clustering and centrality methods, shown to stem from the same optimization problem, to provide a more robust understanding of the SDG interlinkages.
- The development of an innovative visualization tool that leverages the information extracted by clustering and centrality measures to facilitate the interpretation of results.

- The use of the Pareto front to select in each cluster the optimal set of SDG indicators to focus on, ensuring that the most important and impactful indicators are prioritized.

The remainder of this paper is structured as follows: we first review the existing literature on SDG interlinkages in the next Section 2, followed by a detailed presentation of the proposed framework in Section 3, its application to a case study with a discussion of the results and implications in Section 4, and finally, a conclusion including limitations of our work and future research directions in Section 5.

2. Previous works

2.1. SDG interlinkages analysis

Since the launch of the 2030 Agenda in 2015, research on SDG interconnections has grown rapidly, with many studies examining the complex relationships among the 17 goals. The UN emphasizes the principles of universality, indivisibility, and interdependence, highlighting that all SDG are equally important, closely linked, and must be pursued holistically to avoid progress in one area undermining another (Le Blanc, 2015). Given this complexity, diverse methodological approaches have emerged to address the multidimensional challenges involved. These methods can be grouped into the following categories (Fronza et al., 2023; Assubayeva and Marco, 2024): (1) data analysis; (2) expert judgment; (3) modelling; and (4) literature review.

Research on SDG interlinkages has also considered various settings (Fronza et al., 2023; Bennich et al., 2023; Assubayeva and Marco, 2024), including the analysis of interactions: (1) at different levels (indicators, targets, or goals); (2) at distinct spatial scales (national, regional or global); (3) focusing on

a subset of goals (eg. water-energy-food nexus); and (4) with additional external factors (eg. climate).

This paper focuses on data analysis methods that rely on statistical data from official sources, using correlation and network analysis techniques, as illustrated in (Pradhan and Warchold, 2023; Dawes, 2023; Issa et al., 2024). These approaches identify the type and quantify the strength of relationships among variables, enabling the detection of specific synergies and trade-offs. Graph clustering methods help discover groups of variables that form synergy poles, revealing meaningful structures within the complexity of sustainable development. In addition, network analysis can identify central nodes, which represent key areas for intervention that may not be evident through traditional methods. These techniques also enhance the visualization of complex interlinkages, making it easier to understand how multiple variables interact simultaneously. Although other analytical approaches, such as Multiple Factor Analysis (Cling and Delecourt, 2022) and biplots (Cañizares et al., 2022) are of interest, they fall outside the scope of this work. Below, we provide a short review of the main tools used in this paper, including statistical association measures, clustering, and centrality measures.

2.2. Association measures

Research on SDG interlinkages often draws on statistical association measures to assess relationships between variables (indicators, targets or goals). Pearson and Spearman correlation coefficients are commonly used to quantify the direction and strength of linear or monotonic relationships among variables. These pairwise associations can be represented as signed weighted networks. While Pearson is used in studies such as (Lusseau and Mancini, 2019; Swain and Ranganathan, 2021; Wu et al., 2022), others prefer Spear-

man, as in (Pradhan et al., 2017; Kroll et al., 2019; Fonseca et al., 2020; Anderson et al., 2022). However, the Pearson coefficient is sensitive to outliers, assumes linearity, and cannot detect non-linear patterns. The Spearman measure, based on ranks, is more robust for general monotonic trends but is harder to interpret. To capture more complex and non-linear relationships, alternative measures like distance correlation (dCor) (Laumann et al., 2022) and maximal information coefficient (MIC) (Warchold et al., 2021) have been employed. However, they provide only non-negative values and cannot represent trade-off patterns. Table 1 compares the primary characteristics of these correlation coefficients.

Association-based analyses of SDG interlinkages generally follow two approaches: longitudinal and cross-sectional (Pradhan and Warchold, 2023). Longitudinal studies examine how indicators evolve over time within a country or region, identifying dynamic dependencies and potential causal links (Pradhan et al., 2017; Swain and Ranganathan, 2021; Laumann et al., 2022). Cross-sectional studies, by contrast, compare interactions across countries at a single time point, revealing patterns of co-development, regional disparities, and structural dependencies (Kroll et al., 2019; Fonseca et al., 2020; Warchold et al., 2021; Gong et al., 2024).

Method	Type of dependence	Signed	Robustness[1]	Data sensitivity[2]	Interpretability
Pearson	Linear	Yes	Low	High	High
Spearman	Monotonic	Yes	High	Low	Medium
dCor	General	No	Medium	High	Low
MIC	General	No	Medium	High	Low

Table 1: Main characteristics of association measures used for SDG interlinkage analysis

2.3. Graph clustering

Graph clustering is a key tool in SDG interlinkages analysis, helping to uncover structural and functional groupings among goals, targets, or indicators (Weitz et al., 2018). By identifying tightly connected clusters, also referred to as communities or nexuses, clustering supports a more systemic understanding of synergies and trade-offs across domains. Among various methods, modularity-based clustering maximizing within-cluster significant connections (Newman, 2006) is the most widely used approach (Weitz et al., 2018; Swain and Ranganathan, 2021; Laumann et al., 2022; Gong et al., 2024). Spectral clustering, which uses eigenvalue decomposition of the graph Laplacian (see for e.g. (Nascimento and De Carvalho, 2011)), allows for detecting clusters of arbitrary shapes (see for e.g. (Lusseau and Mancini, 2019)). In contrast, standard k-means is less suitable for SDG networks due to its rigid assumptions about cluster number and shape.

2.4. Centrality measures

Centrality measures quantify the influence of vertices based on their position in a network and are widely used across disciplines (see for e.g. (Bloch et al., 2023)). In SDG interlinkages analysis, they help identify the most impactful goals, targets, or indicators (Dawes, 2022, 2023), guiding policymakers in prioritizing high-leverage actions. Different measures capture different aspects of influence. Degree centrality identifies variables with the most direct connections (Pham-Truffert et al., 2020), while betweenness centrality highlights those acting as bridges between otherwise disconnected goals (Gong et al., 2024). Eigenvector centrality (or eigencentrality), by contrast,

[1] Robustness to outliers.
[2] Sensitivity to data scales and distributions.

considers not only a node's connections but also the importance of its neighbors, offering a more nuanced view of systemic influence (Dawes, 2023). Although betweenness can reveal bottlenecks, eigencentrality is generally preferred in SDG analysis due to its ability to identify structurally dominant variables and its greater stability under network changes (Bonacich, 2007).

2.5. Limitation of current approaches

To summarize the previous points, Figure 1 provides a generic overview of commonly used network analysis tools and a general workflow for studying SDG interlinkages.

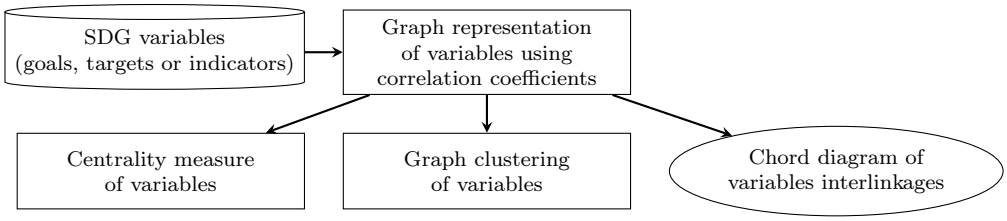

Figure 1: Conventional network analysis procedures for SDG interlinkages.

Within this scope, we identify the following research gaps:

- Existing association measures often lack interpretability for policymakers and overlook key factors such as population size and regional dependencies, limiting acurate representativity at global level.
- Modularity is widely used in graph clustering but is not the only relevant criterion. Moreover, modularity-based algorithms often rely on heuristics, introducing non-determinism and inconsistent community structures.
- While eigenvector centrality has been interpreted for signed directed graphs (Dawes, 2022, 2023), a clear understanding for signed weighted undirected networks in SDG analysis, is still missing.

- Clustering and centrality are typically applied independently, resulting in fragmented insights. Their integration is needed for a coherent understanding of complex systems.
- Representing graphs or networks with chord diagrams, though common, becomes cluttered with many variables or edges, limiting their utility for interpreting complex SDG interlinkages.
- Despite increasing research, no comprehensive framework exists to assist policymakers in designing more actionable interventions by identifying the most critical indicators and the significant positive and negative interactions among them.

In the following section, we introduce our methodology that aims to address the aforementionned issues.

3. Proposed framework

3.1. Overview

Our proposal involves employing complementary tools and methods that ultimately provide a consistent and integrated framework for a robust and enriched analysis of SDG indicators interconnections at a global scale. In Figure 2, we depict the different components of our approach, emphasizing in bold and red the specificities of our methodology in comparison to the base workflow exposed in Figure 1.

In a nutshell, the main features of our approach are the following ones:

- We study interlinkages between SDG at the level of indicators rather than at the level of goals or targets. This approach provides a more granular and precise analysis, ultimately informing more actionable policy design.

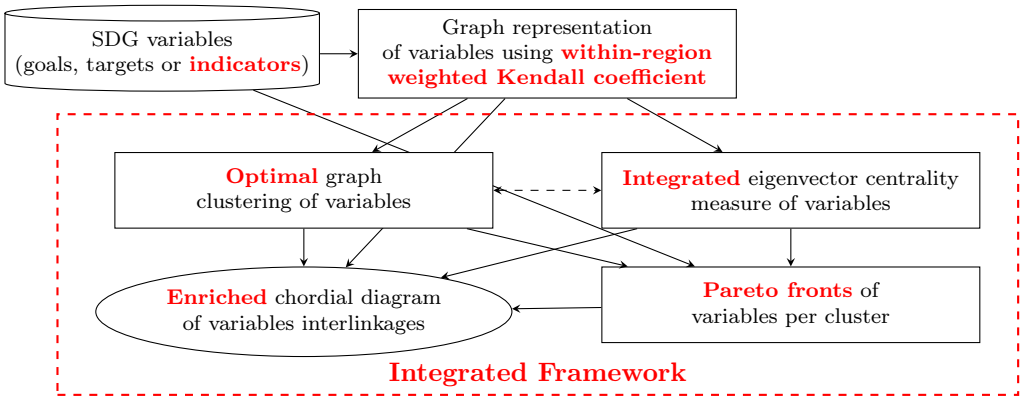

Figure 2: Our consistent and integrated framework for SDG interlinkages analysis and visualization.

- We apply a cross-sectional approach that emphasizes the comparison between countries at a given point in time, with the goal of extracting global structural dependencies among indicators.
- We utilize Kendall coefficient to assess the direction and strength of the relationship between each pair of indicators. Moreover, we take into account the population size of each country as a weight to ensure that the results are representative of the majority of the world's population.
- We emphasize global SDG governance while integrating regional specificities into the strategy. To this end, we extend the weighted Kendall measure to account for regional dependencies, enhancing consistency between regional and global analyses, especially concerning Simpson's paradox.
- We apply an optimal clustering model to the within-region weighted Kendall correlation network to discover clusters of indicators that show strong intra-synergies and strong inter-trade-offs simultaneously.
- We use the principal eigenvector of the within-region weighted Kendall

correlation graph as a centrality measure. This approach is fully aligned with the aforementioned clustering procedure: we show that the leading eigenvector is the solution to a relaxed version of the clustering model.

- In our proposal, the clusters and centrality measures are closely associated, and we use these outputs jointly to represent the SDG indicators in a chord diagram in a structured manner. This feature provides an innovative and informative visualization of the interactions between SDG.
- Studying the interactions at the indicator level allows for a fine-grained analysis, but their large number can be cumbersome. As a result, we propose determining the Pareto front in each cluster by considering two criteria: the percentage of performance and the eigencentrality measure.

In the following paragraphs, we formally introduce and further explain the motivations behind each component of our integrated framework, as well as provide additional details on the complementarities they share. For convenience, a table that lists all notations and definitions employed in the rest of the paper is provided in Appendix A.

3.2. Within-region weighted Kendall correlation

Let X^j and $X^{j'}$ be two indicators, measured across n countries. Denote their value vectors as $\mathbf{x}^j = (x_1^j, \ldots, x_{\mathrm{n}}^j)$ and $\mathbf{x}^{j'} = (x_1^{j'}, \ldots, x_{\mathrm{n}}^{j'})$. For two countries X_i and $X_{i'}$, we introduce the following definitions: $(X_i, X_{i'})$ is concordant[3] if $(x_i^j < x_{i'}^j \wedge x_i^{j'} < x_{i'}^{j'})$ or $(x_i^j > x_{i'}^j \wedge x_i^{j'} > x_{i'}^{j'})$; and $(X_i, X_{i'})$ is discordant[4] if $(x_i^j < x_{i'}^j \wedge x_i^{j'} > x_{i'}^{j'})$ or $(x_i^j > x_{i'}^j \wedge x_i^{j'} < x_{i'}^{j'})$.

[3]A concordant pair $(X_i, X_{i'})$ means that both variables X^j and $X^{j'}$ rank the two individuals X_i and $X_{i'}$ in the same order which indicates a positive association.

[4]A disconcordant pair $(X_i, X_{i'})$ means that the variables X^j and $X^{j'}$ rank the two individuals X_i and $X_{i'}$ in opposite order which indicates a negative association.

Next, to consider all $\frac{\mathrm{n}(\mathrm{n}-1)}{2}$ country pairs, we use the following quantities: $\mathrm{Conc}(\mathbf{x}^j, \mathbf{x}^{j'})$ is the total number of concordant pairs; and $\mathrm{Disc}(\mathbf{x}^j, \mathbf{x}^{j'})$ the total number of discordant pairs. Then Kendall τ_a coefficient is given by:

$$\tau_a(\mathbf{x}^j, \mathbf{x}^{j'}) = \frac{\mathrm{Conc}(\mathbf{x}^j, \mathbf{x}^{j'}) - \mathrm{Disc}(\mathbf{x}^j, \mathbf{x}^{j'})}{\frac{\mathrm{n}(\mathrm{n}-1)}{2}}. \tag{1}$$

τ_a ranges from -1 to 1 (from perfect negative to perfect positive correlation). To account for ties, we introduce the following definitions: $(X_i, X_{i'})$ is tied in $\mathbf{x}^j$ if $x_i^j = x_{i'}^j$; and $\mathrm{Tied}(\mathbf{x}^j)$ denotes the total number of tied pairs in $\mathbf{x}^j$. Accordingly, the adjusted Kendall τ_b is:

$$\tau_b(\mathbf{x}^j, \mathbf{x}^{j'}) = \frac{\mathrm{Conc} - \mathrm{Disc}}{\sqrt{\left(\frac{\mathrm{n}(\mathrm{n}-1)}{2} - \mathrm{Tied}(\mathbf{x}^j)\right)\left(\frac{\mathrm{n}(\mathrm{n}-1)}{2} - \mathrm{Tied}(\mathbf{x}^{j'})\right)}}. \tag{2}$$

Let $\mathbf{S}^j = (s_{ii'}^j)$ of size $\mathrm{n} \times \mathrm{n}$ be the signed matrix of $\mathbf{x}^j$, where: $s_{ii'}^j = -1$ if $x_i^j < x_{i'}^j$; $s_{ii'}^j = 0$ if $x_i^j = x_{i'}^j$; and $s_{ii'}^j = 1$ if $x_i^j > x_{i'}^j$. Then τ_b can be rewritten as:

$$\tau_b(\mathbf{S}^j, \mathbf{S}^{j'}) = \frac{\sum_{i,i'=1}^{\mathrm{n}} s_{ii'}^j s_{ii'}^{j'}}{\sqrt{\sum_{i,i'=1}^{\mathrm{n}} (s_{ii'}^j)^2 \sum_{i,i'=1}^{\mathrm{n}} (s_{ii'}^{j'})^2}}. \tag{3}$$

In contrast to the association measures listed in Table 1, the Kendall measure τ_b has the following properties : it is non-parametric and captures general monotonic association through the concept of concordance and discordance pairwise comparison; it indicates the direction, positive or negative, of the dependence between variables allowing us to represent synergies and trade-off relationships (unlike dCor and MIC); it is highly robust to outliers as it is invariant to positive monotonic transformation of the data; it has low

sensitivity to data scales and distributions since it only relies on the order relations inferred by the variables; it is highly interpretable, as it relies on a logical framework for association that compares the empirical counts of agreement and disagreement when ordering data observations.

Next, to better include global priorities, we use a population-weighted version of Kendall correlation. This approach ensures that indicator associations more accurately represent the current global landscape by giving greater weight to countries with larger populations, thus supporting more equitable and impactful global policy strategies. Integrating population weighting into spatial analysis can lead to confusion, as outlined in (Gluschenko, 2018). In our work, we clearly state that our global analysis operates at the individual level rather than at the country level. Specifically, when randomly selecting an individual from the worldwide population, the varying population sizes of countries determine the sampling probability. Therefore, we propose to weight the concordance and discordance counts with respect to population sizes when computing Kendall coefficient. Weighted versions of the Kendall measure have been studied by several papers (Shieh, 1998; Vigna, 2015). We opt for the following definition denoted by τ_w:

$$\tau_w(\mathbf{S}^j, \mathbf{S}^{j'}) = \frac{\sum_{i,i'} w_i w_{i'} s^j_{ii'} s^{j'}_{ii'}}{\sqrt{\sum_{i,i'} w_i w_{i'} (s^j_{ii'})^2 \sum_{i,i'} w_i w_{i'} (s^{j'}_{ii'})^2}}, \tag{4}$$

where i and i' run across the rows and columns of $\mathbf{S}^j$ or $\mathbf{S}^{j'}$ and w_i is the positive weight of X_i.

The weighted Kendall τ_w coefficient lies in the interval $[-1, 1]$, similar to Kendall τ_a and τ_b, and shares the same interpretations (Vigna, 2015).

In addition, we extend τ_w in order to integrate regional specificities and

make our linkage measure context-dependent. When computing the weighted Kendall measure, we propose to consider only pairs of countries within the same region, rather than all possible country pairs. Our assumption is that assessing the concordance and discordance counts between indicators is more meaningful within a shared regional context, as cross-regional comparisons lack interpretive relevance. From a statistical perspective, our framework explicitly accounts for the dependence of observations, assuming that the region serves as a qualitative variable categorizing countries into homogeneous sub-groups which amounts to a clustered data analysis approach. In fact, regional stratification can address the Simpson's paradox that can be observed in spatial data analysis as exposed in (Sachdeva and Fotheringham, 2023). This phenomenon occurs when a correlation trend apparent in several sub-groups of data, reverses when these groups are aggregated. Suppose that the n countries are partitionned into m regions, $\mathbb{R} = \{\mathbb{R}_1, \ldots, \mathbb{R}_{\mathrm{m}}\}$. We define the within-region weighted (WRW) Kendall coefficient $\tau_{w,\mathbb{R}}$ by:

$$\tau_{w,\mathbb{R}}(\mathbf{S}^j, \mathbf{S}^{j'}) = \frac{\sum_{l=1}^{\mathrm{m}} \sum_{i,i' \in \mathbb{R}_l} w_i w_{i'} s_{ii'}^j s_{ii'}^{j'}}{\sqrt{\sum_{l'=1}^{\mathrm{m}} \sum_{i,i' \in \mathbb{R}_{l'}} w_i w_{i'} (s_{ii'}^j)^2 \sum_{l''=1}^{\mathrm{m}} \sum_{i,i' \in \mathbb{R}_{l''}} w_i w_{i'} (s_{ii'}^{j'})^2}}, \tag{5}$$

where the subscript $i, i' \in \mathbb{R}_l$ is shorthand for $i, i' = 1, \ldots, \mathrm{n}$, such that $X_i \in \mathbb{R}_l \wedge X_{i'} \in \mathbb{R}_l$.

Let us denote by $\mathbf{S}^{j,l} = (s_{ii'}^j)_{i,i' \in \mathbb{R}_l}$, the block submatrix of size $|\mathbb{R}_l| \times |\mathbb{R}_l|$ extracted from $\mathbf{S}^j$ and containing only rows and columns corresponding to countries in region $\mathbb{R}_l$. Then, it is not difficult to see that (5) is similar to:

$$\tau_{w,\mathbb{R}}(\mathbf{S}^j, \mathbf{S}^{j'}) = \sum_{l=1}^{\mathrm{m}} \omega_l \tau_w(\mathbf{S}^{j,l}, \mathbf{S}^{j',l}), \tag{6}$$

where ω_l is the positive weight of region $\mathbb{R}_l$ defined by:

$$\omega_l = \frac{\sqrt{\sum_{i,i' \in \mathbb{R}_l} w_i w_{i'} (s_{ii'}^j)^2 \sum_{i,i' \in \mathbb{R}_l} w_i w_{i'} (s_{ii'}^{j'})^2}}{\sqrt{\sum_{l'=1}^{\mathrm{m}} \sum_{i,i' \in \mathbb{R}_{l'}} w_i w_{i'} (s_{ii'}^j)^2 \sum_{l''=1}^{\mathrm{m}} \sum_{i,i' \in \mathbb{R}_{l''}} w_i w_{i'} (s_{ii'}^{j'})^2}}. \tag{7}$$

Accordingly, $\tau_{w,\mathbb{R}}(\mathbf{S}^j, \mathbf{S}^{j'})$ provides a measure of the direction and intensity of the interaction between X^j and $X^{j'}$ at the global level, while explicitly accounting for population sizes and regional dependencies of countries. It can be interpreted as a linear combination over regions $\mathbb{R}_l$, for $l = 1, \ldots, \mathrm{m}$, of the weighted Kendall association measures $\tau_w(\mathbf{S}^{j,l}, \mathbf{S}^{j',l})$ defined in (4), where each term is weighted by ω_l, which is proportional to the total population of the countries within $\mathbb{R}_l$. Compared to the other methods listed in Table 1, the proposed WRW Kendall measure is the only approach that explicitly incorporates population and regional structures. As we will illustrate later in Paragraph 4.2.1, these features enhance robustness against the Simpson's paradox, that can arise in the case of SDG interlinkages.

In the sequel, we assume a set of p SDG indicators $\{X^1, \ldots, X^{\mathrm{p}}\}$ with observed values over a set of n countries $\{X_1, \ldots, X_{\mathrm{n}}\}$ that are grouped according to m regions $\mathbb{R} = \{\mathbb{R}_1, \ldots, \mathbb{R}_{\mathrm{m}}\}$. Indicators' values are represented by the set of vectors of size n, $\{\mathbf{x}^1, \ldots, \mathbf{x}^{\mathrm{p}}\}$. Our framework is built upon the interlinkages network represented by the signed weighted undirected adjacency matrix $\mathbf{K} = \left(k_{jj'}\right)$ of size $\mathrm{p} \times \mathrm{p}$, where each entry is defined by the WRW Kendall coefficient given in (5). Specifically, $\forall j, j' = 1, \ldots, \mathrm{p}$:

$$k_{jj'} = \tau_{w,\mathbb{R}}(\mathbf{S}^j, \mathbf{S}^{j'}). \tag{8}$$

3.3. Mathematical Relational Analysis clustering

The WRW Kendall correlation matrix **K** captures synergies and trade-offs as positive and negative values. These are represented as a complete graph, with indicators as nodes and signed edge weights reflecting correlation directions and strengths. Figure 3 in page 22 presents a conventional visualization of the SDG indicator network. The indicators are organized with respect to their respective goals. This dense representation with numerous nodes and edges reflects the complexity of sustainability without offering clear insights. To reveal underlying structures and identify key patterns, we apply network analysis tools. To extract synergy poles that are mutually conflicting, we use a graph clustering method that explicitly incorporates both positive and negative associations. It searches for an optimal partition maximizing intra-cluster synergies and inter-cluster tensions. Unlike heuristic approaches, our method formulates the clustering as a binary integer linear program (0-1 ILP), ensuring rigorous and exact solutions.

Our approach builds on the Mathematical Relational Analysis (MRA) framework, originally developed in (Michaud and Marcotorchino, 1979; Marcotorchino, 1986), which combines graph theory, statistics, and optimization to represent association measures and aggregation procedures of binary relations. In our case, the goal is to approximate a graph via an equivalence relation over its nodes. In the MRA notations, a binary relation R over a set of p items is represented by a graph with an adjacency matrix, also called a relational matrix, $\mathbf{R} = (r_{jj'})$ of size p $\times$ p, with the general term: $r_{jj'} = 1$ if $X^j R X^{j'}$, that is X^j is in relation with $X^{j'}$; $r_{jj'} = 0$ otherwise. A clustering (or partition) of the nodes of the graph is exactly the same as an equivalence relation over the set of nodes. This type of binary relations satisfies the following properties: (1) reflexivity,

$\forall j : X^j R X^j$; (2) symmetry, $\forall j \neq j' : X^j R X^{j'} \Leftrightarrow X^{j'} R X^j$; (3) transitivity, $\forall j \neq j' \neq j'' : X^j R X^{j'} \wedge X^{j'} R X^{j''} \Rightarrow X^j R X^{j''}$. In (Michaud and Marcotorchino, 1979), the authors show that all properties can be expressed as linear constraints of terms of the relational matrix $\mathbf{R}$: (1) reflexivity, $\forall j : r_{jj} = 1$; (2) symmetry, $\forall j \neq j' : r_{jj'} = r_{j'j}$; (3) transitivity, $\forall j \neq j' \neq j'' : r_{jj'} + r_{j'j''} - r_{jj''} \leq 1$. We aim to approximate $\mathbf{K}$ using an unknown equivalence relation represented by a relational matrix $\mathbf{R}$. This can be achieved by solving the following 0-1 ILP:

$$\max_{\mathbf{R} \in \{0,1\}^{\mathrm{p} \times \mathrm{p}}} \sum_{j,j'=1}^{\mathrm{p}} k_{jj'} r_{jj'} \text{ s.t. } \begin{cases} r_{jj} = 1, & \forall j, \\ r_{jj'} = r_{j'j}, & \forall j \neq j', \\ r_{jj'} + r_{j'j''} - r_{jj''} \leq 1, & \forall j \neq j' \neq j''. \end{cases} \tag{9}$$

Although clustering is NP-hard, the 0-1 ILP in (9) allows for efficient and exact solutions when p is in the range of tens to a few hundred, as in the case of SDG indicators.

We further detail why Problem (9) enables the detection of indicator clusters that specifically reveal synergies and trade-offs within the SDG network. For simplicity, and without loss of generality, assume that there are no tied values in any of the vectors $\mathbf{x}^j$, $j = 1, \ldots, \mathrm{p}$. In this case, $k_{jj'}$ from (8) can be written as the difference between the estimated probability that X^j and $X^{j'}$ are concordant and the estimated probability that they are discordant: $k_{jj'} = \widehat{P}(\mathrm{Conc}(X^j, X^{j'})) - \widehat{P}(\mathrm{Disc}(X^j, X^{j'}))$. Then, it is not difficult to see that the objective function in Problem (9) is equivalent to: $\max_{\mathbf{R} \in \{0,1\}^{\mathrm{p} \times \mathrm{p}}} \sum_{j,j'=1}^{\mathrm{p}} \widehat{P}(\mathrm{Conc}(X^j, X^{j'})) r_{jj'} + \sum_{j,j'=1}^{\mathrm{p}} \widehat{P}(\mathrm{Disc}(X^j, X^{j'}))(1 - r_{jj'})$. From this formulation, we observe that: (1) indicators X^j and $X^{j'}$ are likely to be in the same cluster ($r_{jj'} = 1$) when $\widehat{P}(\mathrm{Conc}(X^j, X^{j'}))$ exceeds

$\widehat{P}(\text{Disc}(X^j, X^{j'}))$, reflecting potential synergies; and (2) conversely, when $\widehat{P}(\text{Disc}(X^j, X^{j'}))$ dominates, X^j and $X^{j'}$ tend to be assigned to different clusters ($r_{jj'} = 0$), indicating trade-off dynamics. This type of reasoning is typical of the MRA methodology. The specific case of Problem (9) is a conventional MRA clustering model (Marcotorchino and Michaud, 1981) and it is clearly aligned with the dual objective in SDG interlinkages of discovering clusters that exhibit positive synergies while simultaneously showing strong negative correlations with each other.

Note that similar ideas have been re-discovered in the context of correlation clustering (see for e.g. (Wahid and Hassini, 2022)). More precisely, the impactful paper (Demaine et al., 2006) that applies the correlation clustering framework to general weighted graphs relies on a 0-1 ILP that is equivalent to Problem (9). We demonstrate this equivalence in Appendix B. However, we refer to the MRA framework due to its precedence.

3.4. Eigenvector centrality and MRA clustering with two clusters

In addition to graph clustering, centrality measures are other tools borrowed from network analysis to extract meaningful information from the SDG interactions graph. They allow highlighting nodes that are most strongly connected to others and, thus, most likely to have a ripple effect on the achievement of multiple SDG.

Let $\mathbf{K} = (k_{jj'})$ be a given correlation matrix between the indicators X^j with $j = 1, \ldots, \text{p}$. We denote by $\mathbf{v} = (v_j)$ the vector of size p that gives the centrality measure for each indicator X^j. We focus on eigenvector centrality which quantifies the global influence of a node X^j across the entire network

structure. It is formally defined as follows, $\forall j$:

$$v_j = \frac{1}{\lambda} \sum_{j'=1}^{\mathrm{p}} k_{jj'} v_{j'}, \tag{10}$$

where $\lambda > 0$ is interpreted as a scaling factor.
Eigenvector centrality is based on the idea that v_j, the importance of X^j, is determined by the importance of its neighboring nodes. Specifically, the contribution of each neighbor $X^{j'}$, with importance $v_{j'}$, is weighted by the strength of their connection, represented by $k_{jj'}$.

From a mathematical standpoint, the correlation matrix $\mathbf{K}$ being a real symmetric square matrix of size $\mathrm{p} \times \mathrm{p}$, it has p real eigenvalues $\lambda_1 \geq \lambda_2 \geq \ldots \geq \lambda_\mathrm{p}$ associated to p eigenvectors $\mathbf{v}^1, \mathbf{v}^2, \ldots, \mathbf{v}^\mathrm{p}$ that are mutually orthogonals and by definition we have, $\forall j : \mathbf{K}\mathbf{v}^j = \lambda_j \mathbf{v}^j$. Then, the eigenvector centrality $\mathbf{v}$ and the scaling factor λ in (10) are exactly the principal eigenvector and eigenvalue $\mathbf{v}^1$ and λ_1: $\mathbf{v} = \mathbf{v}^1$ and $\lambda = \lambda_1$.

Eigencentrality is typically applied to binary or non-negative weighted adjacency matrices. In such regular cases, the Perron–Frobenius theorem ensures that both the leading eigenvalue λ_1 and its corresponding eigenvector $\mathbf{v}^1$ have non-negative entries, allowing for a straightforward ranking of nodes by importance. This approach has been used in SDG correlation networks in (Swain and Ranganathan, 2021; Laumann et al., 2022).

In the more general case where $\mathbf{K}$ contains both positive and negative values, it is not guaranteed that λ_1 and $\mathbf{v}^1$ contain non-negative values. In this situation, if some nodes have a negative centrality measure, the definition of eigencentrality provided by (10) is more difficult to interpret. In (Bonacich and Lloyd, 2004), the authors address this concern in the context of social network analysis and show that, in the case of a signed adjacency matrix

with "like" (+1) *versus* "dislike" (-1) relationships, the leading eigenvector $\mathbf{v}^1$ reveals two groups of nodes: those with positive values in $\mathbf{v}^1$, which are opposed to those with negative values, forming two contrasting cliques.

Let $\mathbf{K}$ be a signed weighted undirected adjacency matrix. Then we have the following properties whose proofs are given in Appendix C.

Lemma 1. *The MRA clustering Problem* (9) *with the additional constraint that* $\mathbf{R}$ *encodes a partition with two clusters is equivalent to the discrete optimization problem* $\max_{\check{\mathbf{z}} \in \{-1,1\}^{\mathrm{p}}} \check{\mathbf{z}}^\top \mathbf{K} \check{\mathbf{z}}$*, where* $\check{\mathbf{z}}^\top$ *is the transpose of* $\check{\mathbf{z}}$*.*

Lemma 2. $\mathbf{K}$*'s leading eigenvector* $\mathbf{v}^1$ *is the optimal solution of the continuous relaxation of the MRA clustering Problem* (9) *with two clusters* $\max_{\tilde{\mathbf{z}} \in \mathbb{R}^{\mathrm{p}}} \tilde{\mathbf{z}}^\top \mathbf{K} \tilde{\mathbf{z}}$ *subject to* $\|\tilde{\mathbf{z}}\|^2 = 1$*, where* $\|.\|$ *is the Euclidean norm in* $\mathbf{R}^{\mathrm{p}}$*.*

Proposition 1. $\mathbf{K}$*'s leading eigenvector* $\mathbf{v}^1$ *encodes an approximate solution of the MRA clustering Problem* (9) *with the additional constraint of a partition with two clusters. Specifically, the two subsets are identified by the signed vector derived from* $\mathbf{v}^1$*.*

These properties demonstrate that eigencentrality vector $\mathbf{v} = \mathbf{v}^1$, derived from a signed weighted undirected graph $\mathbf{K}$ has the following interpretations: (1) the signs make it possible to identify two main poles; (2) the absolute values provide a measure of the influence of the nodes; and (3) the vertices that have highly positive and highly negative values are the ones that are the most in trade-off. Thereby, contrary to an unsigned network, eigenvector centrality on a signed network results in a preference ordering of vertices on a bipolar scale with two opposing extremes, providing richer information extraction.

For completeness, we demonstrate in Appendix D that subsequent eigenvectors of $\mathbf{K}$ are strongly associated with clustering nodes into more than

two groups. However, our contribution focuses on operational decisions that require simplifying the inherent complexity of a network into interpretable tools. Therefore, our framework restricts itself to the principal eigenvector instead of exploiting the full spectrum.

Furthermore, the MRA clustering identifies groups of vertices without requiring prior knowledge of the optimal number of clusters. For practical applications like SDG interlinkage analysis with a few tens or low hundreds of variables, the 0-1 ILP (9) can be solved optimally within reasonable processing times (see Appendix F). Among detected clusters, two are strongly opposed, revealed by extreme eigencentrality values, while remaining clusters lie between these poles, providing finer-grained analysis. The MRA clustering and eigencentrality outputs are in fact complementary. In the following Subsection, we introduce a visualization tool that integrates both outputs.

3.5. Visualization tool

In Figure 3, we provide illustrations of chord diagrams of the SDG interconnections graph between a set of 96 indicators measured by our approach. The intensity of the edge color indicates the strength of the relationship given by the WRW Kendall correlation measure. On the left hand side, only the positive correlation measures (in red) are illustrated while, on the right hand side, solely the negative association values (in gray) are depicted. In Figure 3, the indicators are organized in circle with respect to the 17 goals they belong to, from sdg1 to sdg17. From these graphs, it is difficult to infer any meaningful insights because there are too many edges that cross each other, creating a cluttered representation.

In contrast, the connection we have established previously between MRA clustering and eigenvector centrality can serve as a framework to reorganize

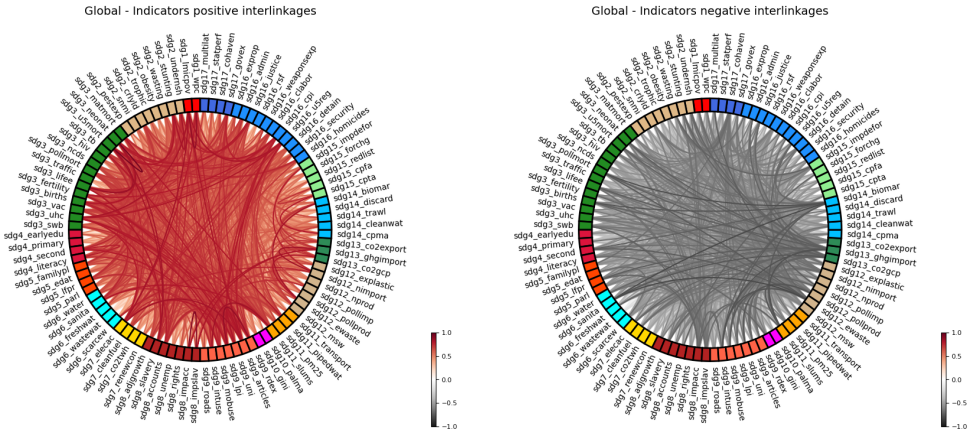

Figure 3: Chord diagrams of the SDG interlinkages of the 96 indicators organized with respect to their goals. Left: positive correlations only (in red). Right: negative correlations only (in gray). The darker the color, the stronger the interconnection.

the indicators and provide a more informative visualization of the SDG interlinkages using chord diagrams: (1) firstly, we can group indicators based on the clusters identified by the MRA clustering; (2) secondly, we can arrange the clusters in a circular order, starting from the top and moving counterclockwise, according to the mean eigencentrality measures; and (3) thirdly, within each cluster, we can order the indicators according to their eigenvector centrality scores. Therefore, indicators in the top left and the ones in the top right positions are those that tend to be the most in trade-off with each other. In Figure 4, we depict the chord diagrams that use the reorganization we have just described. This visualization provides more meaningful information. The left diagram illustrates two clusters that represent the two poles of synergy. The density of positive intraconnections is sharply indicated, and the intensity of the color helps identify the most influential indicators in each group. The right diagram displays the trade-offs between indicators within

the two clusters. It also shows that the indicators in the top left and top right positions exhibit strong opposite correlations.

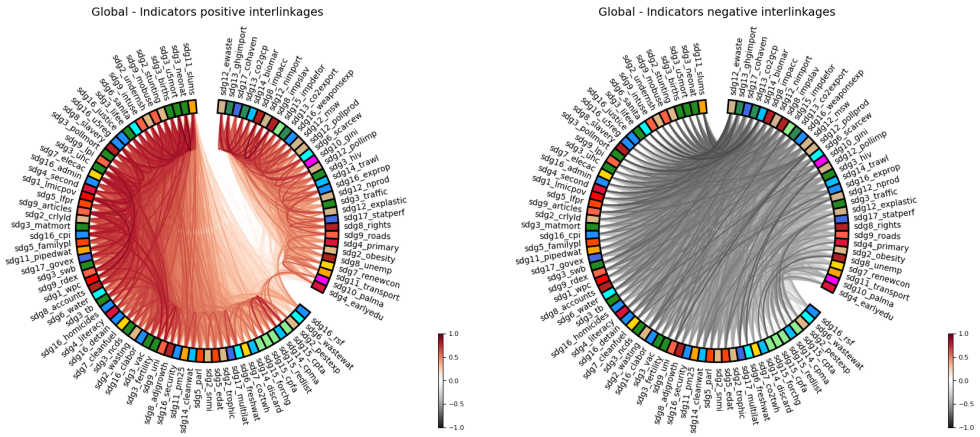

Figure 4: Chord diagrams of the SDG interlinkages of the 96 indicators organized with respect to their two clusters and eigencentrality scores. Left: positive correlations only (in red). Right: negative correlations only (in gray). The darker the color, the stronger the interconnection.

In summary, our approach extracts meaningful grouping and ranking structures from the WRW Kendall association graph, enhancing chord diagram visualizations. It reveals clusters of indicators that are positively interlinked, helping to identify key synergies, while also exposing trade-offs between groups, clarifying the complex interdependencies among SDG and the development dilemmas they represent. These clusters often span multiple goals, emphasizing the need for integrated policy strategies. Recognizing such patterns allows decision-makers to foster more coherent and sustainable policy design. More detailed interpretations are provided in Section 4.

3.6. Decision aiding using Pareto fronts

Our focus is on exploring the relationships between SDG through their individual indicators rather than through broader goals or targets. While this

detailed perspective enables us to gain a clearer insight, it necessitates the manipulation of numerous variables, which complicate the analysis process. To address this issue, we propose focusing on two complementary criteria to select the indicators that decision-makers should prioritize. The first criterion U is the percentage of performance (or achievement) of indicators and the second criterion V is the eigencentrality measure introduced in Paragraph 3.4. The criterion U is based on indices defined in (Sachs et al., 2024; Lafortune et al., 2018) and provided by the SDR 2024 dataset. This dataset, introduced in more details in Section 4, serves as the primary source for our empirical analysis and supports the application of our integrated framework. It provides us with censored and normalized values x_i^j in the range $[0, 100]$ indicating the percentage of achievement of country X_i for SDG indicator X^j. Since our analysis is conducted at the global scale, the first criterion U is the weighted mean of the percentages of performance across all countries, using population size as the weighting scheme.

Then, to facilitate a more focused and interpretable analysis, we reduce the number of SDG indicators using the concept of the Pareto front. Widely used in multi-objective optimization, the Pareto front represents the set of non-dominated solutions that balance multiple criteria. In our case, we apply this concept from a bi-objective perspective, selecting indicators that are simultaneously underperforming and influential. Specifically, an indicator is said to be Pareto optimal if there is no other indicator that improves U without degrading V, or *vice versa*. Let us denote $\mathbf{u} = (u_j)$ with $u_j = \sum_{i=1}^{\mathrm{n}} w_i x_i^j$, the vector of the weighted means of percentages of performance and $\mathbf{v} = (v_j)$ the vector of eigenvector centrality measures. Regarding U, X^j should be prioritized over $X^{j'}$ if $u_j < u_{j'}$, because in that case, X^j has a low level of advancement. On the contrary, in the case of V, X^j should

be prioritized over $X^{j'}$ if $|v_j| > |v_{j'}|$, since this indicates that X^j is more influential. Accordingly, we say that an SDG indicator X^j is Pareto optimal if and only if there is no other $X^{j'}$ that is strictly preferred for both criteria.

The Pareto front is defined as the subset of indicators that are Pareto optimal. In our approach, we determine the Pareto front for each cluster rather than for the overall set of indicators. This procedure aligns with the structured insights provided by our MRA clustering and integrated eigenvector centrality. First, it allows for broader coverage of the main poles of synergies, capturing unique interconnections within each cluster. Second, this approach enhances our ability to identify critical trade-offs between clusters. In Figure 5, we present the SDG interlinkages chordal graphs shown in Figure 4, but restricted to the Pareto fronts of each cluster. In this case, the number of indicators is decreased from 96 to 13.

To sum up, our framework significantly reduces the systemic complexity of sustainable development, enabling decision-makers to concentrate on core operational dimensions. By narrowing down to the most critical indicators, policymakers are equipped to target more specific actions that are actionable, rather than being overwhelmed by a broader set of targets or goals, which can often lack clarity in implementation. In the next subsection, we discuss our empirical study in greater depth.

4. Application to the SDR 2024 dataset

4.1. The SDR 2024 dataset

Similarly to (Kroll et al., 2019; Fonseca et al., 2020; Wu et al., 2022), we analyze SDG interlinkages using the SDR 2024 dataset provided by the Sus-

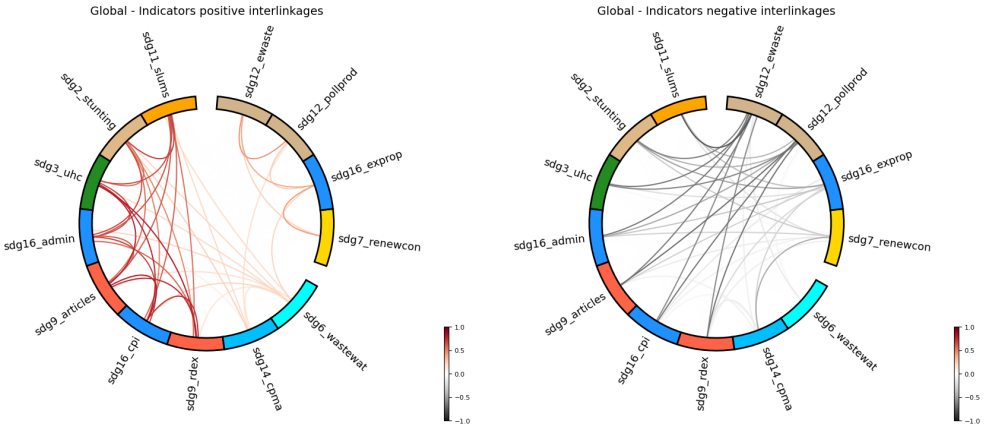

Figure 5: Chord diagrams of the SDG interlinkages of the indicators in the Pareto fronts organized with respect to their two clusters and eigencentrality scores. Left: positive correlations only (in red). Right: negative correlations only (in gray). The darker the color, the stronger the interconnection.

tainable Development Solutions Network[5] (SDSN). The SDSN publishes an annual report which assesses the progress of countries toward achieving the SDG. The SDR 2024 dataset[6] serves as the foundation for the SDSN report of 2024 (Sachs et al., 2024). We apply our framework to this dataset and to integrate context-specific dependencies in our WRW Kendall association measure given by (5), we considered the 7 regions as defined in the SDSN report, which consist of the following: Eastern Europe & Central Asia, East & South Asia, Latin America and the Caribbean, Middle East and North Africa, Oceania, OECD members, Sub-Saharan Africa.

The SDR 2024 dataset countains 100 global indicators and 193 countries.

[5]SDSN is a global initiative launched by the UN to promote practical solutions for sustainable development.

[6]This dataset is freely available at `https://dashboards.sdgindex.org/downloads`. Descriptions of all indicators, along with their corresponding worst-case and best-case scenario thresholds, are provided in (Sachs et al., 2024) and in the SDR 2024 dataset spreadsheet file.

We work with the censored and normalized version of these variables as described in Paragraph 3.6 and Appendix E as well. These motivated data preprocessing steps performed by the SDSN ensure the homogeneity of variables, significantly enhancing the clarity and reproducibility of the analyses conducted. However, there are many missing values. We implemented the following extra procedures to address this issue: (1) if an indicator has more than 40% missing values, it is dropped; (2) then, if a country has more than 30% missing values, it is removed; (3) finally, we impute remaining missing values using a conventional nearest neighbors method. Specifically, we replace any missing value X^j of country X_i by the mean of X^j over the three nearest neighbors of X_i. After this first round of filtering, we were left with only two countries from the region of Oceania. We decided to remove these two cases for statistical consistency reasons. Consequently, our final dataset consists of 96 indicators and 165 countries, distributed across 6 regions.

4.2. Empirical results

Let $\mathbf{X} = (x_i^j)$ be the data matrix of size 165×96, where $i = 1, \ldots, 165$ and $j = 1, \ldots, 96$. For all pairs of vectors $\mathbf{x}^j = (x_i^j)$ and $\mathbf{x}^{j'} = (x_i^{j'})$, we applied (5) to assess the interlinkage between indicators X^j and $X^{j'}$, resulting in the WRW Kendall correlation matrix $\mathbf{K}$ of size 96×96. In Paragraph 4.2.1, we provide an example that underscores the relevance of the WRW Kendall measure regarding the Simpson's paradox. Then, in Paragraph 4.2.2, we discuss the results of applying our analytical framework to $\mathbf{K}$, including MRA clustering, eigencentrality, structured chord diagrams and selection of cluster-specific Pareto optimal indicators.

4.2.1. Illustration of the WRW Kendall measure

To illustrate the impact of the WRW extension of the Kendall coefficient, we consider the following pair of indicators : X^j = sdg1_wpc, "Poverty headcount ratio at \$2.15/day (2017 PPP, %)"; and $X^{j'}$ = sdg3_traffic, "Traffic deaths (per 100,000 population)". For this pair of variables, the distribution of values $\mathbf{x}^j$ and $\mathbf{x}^{j'}$ across all countries yields a weighted Kendall correlation, given by (4), of 0.24. Unlike this positive association, our WRW Kendall correlation, which accounts for regional dependencies as defined by (5) or (6), is negative, with a value of -0.48. The region-specific weighted Kendall scores $\tau_w(\mathbf{S}^{j,l}, \mathbf{S}^{j',l})$, with l indexing the 6 regions, are the following ones: (1) 0.18 for Eastern Europe & Central Asia; (2) -0.60 for East & South Asia; (3) 0.06 for Latin America and the Caribbean; (4) -0.10 for Middle East and North Africa; (5) 0.03 for OECD members; (6) -0.19 for Sub-Saharan Africa.

This serves as a compelling illustration of Simpson's paradox, where the weighted Kendall correlation measured at global scale shows a positive overall trend but reveals significant contradictions when analyzed within specific regions. The positive weighted Kendall association suggests a synergy between reducing poverty and lowering traffic deaths. In contrast, the negative within-region correlation, which we emphasize, underscores the complexity of these relationships, highlighting that this global association does not hold when accounting for regional dependencies. Spatio-temporal heterogeneity and changing variation in the relationship between economic development and road traffic death in East & South Asia have already been outlined in several research works (see for e.g. (Chan et al., 2025)).

This discrepancy exemplifies the importance of considering localized dy-

namics to avoid misleading conclusions that could arise from aggregating data. In this regard, our WRW Kendall measure highlights the role of regional dependencies as suggested by previous SDG interlinkages studies (see for e.g. (Laumann et al., 2022)).

4.2.2. Results of our framework

To structure the signed weighted network $\mathbf{K}$, we solve the MRA clustering Problem (9). The optimal solution yields two clusters. As detailed in Section 3.4, the sign of the entries in the leading eigenvector $\mathbf{v}^1$ of $\mathbf{K}$ aligns exactly with this partition, linking eigencentrality and clustering outcomes. We then reorder the indicators based on the MRA clustering and eigenvector centrality, as described in Section 3.5. This produces clearer and more informative chord diagrams as shown in Figure 4[7].

In addition, we analyzed the weighted Kendall networks with linkage measures given by $\tau_w(\mathbf{S}^{j,l}, \mathbf{S}^{j',l})$ as defined in (4), with l indexing the 6 regions. Since our primary focus is on the global scale, we do not discuss these regional results. However, the related MRA clustering processing times and structured chord diagrams exhibiting more thant two optimal clusters are respectively included in Appendix F and the supplementary materials for the interested reader.

Despite improved visualization and partial simplification, the large number of indicators still challenges decision-making. To address this, we identify the Pareto front for each cluster to retain only the most relevant indicators. Figure 5 displays the interlinkage subgraph between these selected indicators. The WRW Kendall correlation submatrix for the indicators on the Pareto

[7] All indicator acronyms, descriptions, and eigencentrality scores are provided in the supplementary materials.

front of each cluster and the related population weighted mean performance percentages U, and eigencentrality measures V are provided in Appendix G.

In summary, our framework facilitates more actionable interventions for the SDG by identifying core indicators for efficient systemic improvement. Moreover, instead of designing policy plans based on 96 indicators, our approach enables reducing the complexity of sustainable development by selecting a smaller subset of 13 key variables.

4.3. Results interpretations

In the following paragraphs, we briefly interpret the results we obtained for each cluster-specific Pareto front. The cited correlation and criteria values are provided in Appendix G. Note that more detailed interpretations are given in the supplementary materials for the interested reader.

4.3.1. Pareto-Cluster 1:

This Pareto-Cluster encompasses governance quality, innovation capacity, and health and social development (sdg16, sdg11, sdg9, sdg3, sdg2), with high-positive correlations ($\tau_{w,\mathbb{R}} > 0.6$) suggesting a virtuous cycle where progress in one area reinforces others.

Strong governance with low corruption and high administrative efficiency correlates with increased R&D investment (0.72 and 0.68) and scientific output (0.79 and 0.60). These governance indicators also correlate with universal health coverage at 0.76 and 0.66, indicating transparent institutions enhance both research and health service delivery (Acemoglu and Robinson, 2013; Rocha, 2019). R&D expenditure and scientific output each show strong correlations (0.78) with universal health coverage, demonstrating that research investments improve health outcomes.

Urban conditions and nutrition are linked through infrastructure: slum prevalence (sdg11_slums) correlates with child stunting (sdg2_stunting) at 0.69. Without safe housing, clean water, and sanitation, health advances are hampered (Silva et al., 2023). Anthropogenic wastewater treatment currently reaches only 13.13% of achievement, indicating urgent infrastructure needs. Clean water access and proper wastewater management are essential for health, reducing inequalities, and sustainable growth.

4.3.2. Pareto-Cluster 2:

This Pareto-Cluster captures institutional capacity, environmental sustainability, and resource efficiency (sdg16, sdg12, sdg7) with moderately strong positive correlations (0.4 range), indicating progress in one facet accompanies progress in others.

Pollution and waste management are coupled at 0.44: countries limiting industrial pollution (sdg12_pollprod) also tend to manage electronic waste (sdg12_ewaste) effectively, suggesting general environmental responsibility. E-waste emerges as the most central node in this Pareto-Cluster and is a critical leverage point for sustainability.

Rule-of-law frameworks significantly impact waste governance and renewable energy adoption. Secure property rights (sdg16_exprop) correlate with better e-waste recycling (0.37) and higher renewable energy use (0.43) (Hoicka et al., 2021). Strengthening institutions is essential for circular economy practices. Renewable energy consumption (sdg7) and property rights (sdg16) are Pareto optimal but underperforming at 20.07% and 27.34%, respectively, marking them as urgent global policy priorities.

4.3.3. Cross-Cluster Trade-offs

Critical negative interactions exist between Pareto-Clusters, especially between social development and environmental sustainability. The strong negative correlation of -0.77 between slum prevalence (sdg11_slums) and e-waste generation (sdg12_ewaste) reflects a development paradox: urban upgrades increase electronic consumption and e-waste despite reducing slums. This underscores the need to pair urban development with circular economy strategies such as urban mining (Ouro-Salim, 2024).

Inverse relationships exist between scientific output (sdg9_articles) and research investments (sdg9_rdex) *versus* industrial pollution (sdg12_pollprod) at -0.69 and -0.67 respectively, suggesting rapid industrialization drives emissions without stringent environmental controls. Universal health coverage (sdg3_uhc) and waste generation (sdg12_ewaste) correlate negatively at -0.65, as broader health coverage increases consumption and medical equipment waste (Ogunseitan, 2022).

These trade-off pairs act as caution flags requiring inter-sectoral coordination. Investments in R&D (sdg9) should pair with green technology research and pollution regulation (sdg12), while healthcare expansions (sdg3) should integrate sustainability measures.

5. Conclusion and future works

This paper presents a data-driven framework for analyzing SDG interlinkages at the indicator level. By extending Kendall correlation to incorporate population weighting and regional specificity, and integrating clustering and centrality measures, our framework captures both synergies and trade-offs. Pareto fronts and visualization tools equip decision-makers with

mechanisms to prioritize high-impact indicators, supporting more coherent global sustainability governance.

Empirical results reveal strong interlinkages between governance quality, innovation, and health outcomes, suggesting effective institutions foster research ecosystems and equitable health services. The analysis highlights links between urban conditions, nutrition, and clean water access, reinforcing infrastructure's foundational role. Environmental sustainability is tied to institutional strength, with better rule-of-law supporting pollution control, waste management, and renewable energy. However, critical trade-offs emerge: improvements in living standards correlate with increased electronic waste and industrial emissions, underscoring the need for integrated strategies balancing socio-economic progress with environmental stewardship.

Several limitations merit acknowledgment. First, our analysis relies on the SDR 2024 database, which may reflect dataset-specific biases. Future work will apply our methodology to additional global databases from the UN and World Bank to robustify findings. Second, our framework identifies cross-sectional correlations rather than causal relationships. Deeper analyses using time series data and Granger causality will explore causal dynamics. Third, although our framework accounts for regional context, the analysis remains primarily global. Future research will extend the method to national or regional levels.

Finally, while motivated by SDG interconnections, the proposed framework could be applied to any context involving signed weighted graphs, including social influence networks, biological systems, and financial networks. In that perspective, for large-scale instances, heuristic procedures can replace exact optimization, preserving scalability while maintaining the benefits of our approach.

Acknowledgment

We would like to express our gratitude to the two anonymous referees for their valuable insights and constructive feedback, which significantly contributed to the improvement of this manuscript.

This work is supported by the Agence Nationale de la Recherche of the French government through the program "Investissements d'Avenir" ANR-10-LABX-14-01.

This project is funded by the International Research Center for Disaster Sciences and Sustainable Development of the I-SITE initiative led by the University of Clermont Auvergne.

References

Acemoglu, D., Robinson, J.A., 2013. Why nations fail: The origins of power, prosperity, and poverty. Crown Currency.

Ah-Pine, J., 2022. Learning doubly stochastic and nearly idempotent affinity matrix for graph-based clustering. European Journal of Operational Research 299, 1069–1078.

Anderson, C.C., Denich, M., Warchold, A., Kropp, J.P., Pradhan, P., 2022. A systems model of SDG target influence on the 2030 agenda for sustainable development. Sustainability science 17, 1459–1472.

Assubayeva, A., Marco, J., 2024. Methodological approaches on synergies and trade-offs within the 2030 agenda. iScience 27.

Bennich, T., Persson, Å., Beaussart, R., Allen, C., Malekpour, S., 2023. Recurring patterns of SDG interlinkages and how they can advance the 2030 agenda. One Earth 6, 1465–1476.

Bloch, F., Jackson, M.O., Tebaldi, P., 2023. Centrality measures in networks. Social Choice and Welfare 61, 413–453.

Bonacich, P., 2007. Some unique properties of eigenvector centrality. Social networks 29, 555–564.

Bonacich, P., Lloyd, P., 2004. Calculating status with negative relations. Social networks 26, 331–338.

Cañizares, J.F.R., Galindo, P.V., Phillis, Y., Grigoroudis, E., 2022. Graphical sustainability analysis using disjoint biplots. Operational Research 22, 1575–1596.

Chan, J., Li, Q., Shi, T., 2025. How economic development impacts transportation safety: Evidence from china. Transport Policy 171, 428–439.

Cling, J.P., Delecourt, C., 2022. Interlinkages between the sustainable development goals. World Development Perspectives 25, 100398.

Dawes, J., 2022. SDG interlinkage networks: Analysis, robustness, sensitivities, and hierarchies. World Development 149, 105693.

Dawes, J.H., 2023. Network analysis of SDG interlinkages, in: Interlinkages between the Sustainable Development Goals. Edward Elgar Publishing, pp. 94–128.

Demaine, E.D., Emanuel, D., Fiat, A., Immorlica, N., 2006. Correlation clustering in general weighted graphs. Theoretical Computer Science 361, 172–187.

Ding, C., He, X., 2004. K-means clustering via principal component analysis,

in: Proceedings of the twenty-first international conference on Machine learning, p. 29.

Fan, K., 1949. On a theorem of weyl concerning eigenvalues of linear transformations i. Proceedings of the National Academy of Sciences 35, 652–655.

Fonseca, L.M., Domingues, J.P., Dima, A.M., 2020. Mapping the sustainable development goals relationships. Sustainability 12, 3359.

Forrest, J., Lougee-Heimer, R., 2005. CBC user guide, in: Emerging theory, methods, and applications. INFORMS, pp. 257–277.

Fronza, V., Barbero Vignola, G., Borchardt, S., Valentini, S., Buscaglia, D., Maroni, M., Marelli, L., 2023. Uncovering SDG interlinkages: interconnection at the core of the 2030 agenda. Publications Office of the European Union .

Fuso Nerini, F., Mazzucato, M., Rockström, J., Van Asselt, H., Hall, J.W., Matos, S., Persson, Å., Sovacool, B., Vinuesa, R., Sachs, J., 2024. Extending the sustainable development goals to 2050—a road map. Nature 630, 555–558.

Gluschenko, K., 2018. Measuring regional inequality: to weight or not to weight? Spatial economic analysis 13, 36–59.

Gong, M., Yu, K., Xu, Z., Xu, M., Qu, S., 2024. Unveiling complementarities between national sustainable development strategies through network analysis. Journal of Environmental Management 350, 119531.

Hoicka, C.E., Lowitzsch, J., Brisbois, M.C., Kumar, A., Camargo, L.R., 2021. Implementing a just renewable energy transition: Policy advice for

transposing the new european rules for renewable energy communities. Energy Policy 156, 112435.

Issa, L., Mezher, T., El Fadel, M., 2024. Can network analysis ascertain SDGs interlinkages towards evidence-based policy planning? a systematic critical assessment. Environmental Impact Assessment Review 104, 107295.

Kroll, C., Warchold, A., Pradhan, P., 2019. Sustainable development goals (SDGs): Are we successful in turning trade-offs into synergies? Palgrave Communications 5.

Lafortune, G., Fuller, G., Moreno, J., Schmidt-Traub, G., Kroll, C., 2018. SDG index and dashboards detailed methodological paper .

Laumann, F., von Kügelgen, J., Uehara, T.H.K., Barahona, M., 2022. Complex interlinkages, key objectives, and nexuses among the sustainable development goals and climate change: a network analysis. The Lancet Planetary Health 6, e422–e430.

Le Blanc, D., 2015. Towards integration at last? the sustainable development goals as a network of targets. Sustainable Development 23, 176–187.

Lusseau, D., Mancini, F., 2019. Income-based variation in sustainable development goal interaction networks. Nature Sustainability 2, 242–247.

Marcotorchino, F., 1986. Cross association measures and optimal clustering, in: COMPSTAT: Proceedings in Computational Statistics, 7th Symposium held in Rome 1986, Springer. pp. 188–194.

Marcotorchino, J., Michaud, P., 1981. Heuristic approach of the similarity aggregation problem. Methods of operations research 43, 395–404.

Michaud, P., Marcotorchino, F., 1979. Modèles d'optimisation en analyse des données relationnelles. Mathématiques et Sciences humaines 67, 7–38.

Mitchell, S., OSullivan, M., Dunning, I., 2011. Pulp: a linear programming toolkit for python. The University of Auckland, Auckland, New Zealand 65, 25.

Nascimento, M.C., De Carvalho, A.C., 2011. Spectral methods for graph clustering–a survey. European Journal of Operational Research 211, 221–231.

Newman, M.E., 2006. Modularity and community structure in networks. Proceedings of the national academy of sciences 103, 8577–8582.

Nilsson, M., Weitz, N., 2019. Governing trade-offs and building coherence in policy-making for the 2030 agenda. Politics and Governance 7, 254–263.

Ogunseitan, O.A., 2022. Side effects of the electronic health care revolution: Toxic e-waste. World Neurosurgery 167, 2–3.

Ouro-Salim, O., 2024. Urban mining of e-waste management globally: Literature review. Cleaner Waste Systems , 100162.

Peng, J., Wei, Y., 2007. Approximating k-means-type clustering via semidefinite programming. SIAM journal on optimization 18, 186–205.

Pham-Truffert, M., Metz, F., Fischer, M., Rueff, H., Messerli, P., 2020. Interactions among sustainable development goals: Knowledge for identifying multipliers and virtuous cycles. Sustainable development 28, 1236–1250.

Pradhan, P., Costa, L., Rybski, D., Lucht, W., Kropp, J.P., 2017. A system-

atic study of sustainable development goal (SDG) interactions. Earth's Future 5, 1169–1179.

Pradhan, P., Warchold, A., 2023. Quantitative approaches to explore synergies and trade-offs among sustainable development goals (sdgs), in: Interlinkages between the Sustainable Development Goals. Edward Elgar Publishing, pp. 70–93.

Pradhan, P., Weitz, N., Daioglou, V., Abrahão, G.M., Allen, C., Ambrósio, G., Arp, F., Asif, F., Bennich, T., Benton, T.G., et al., 2024. Three foci at the science-policy interface for systemic sustainable development goal acceleration. Nature communications 15, 8600.

Rocha, L.A., 2019. Corruption, bureaucracy and other institutional failures: the "cancer" of innovation and development. Economics bulletin 39.

Sachdeva, M., Fotheringham, A.S., 2023. A geographical perspective on Simpson's paradox. Journal of Spatial Information Science , 1–25.

Sachs, J.D., Lafortune, G., Fuller, G., 2024. The SDGs and the UN summit of the future. Sustainable development report 2024. Dublin: Dublin University Press. doi:doi:10.25546/108572.

Shieh, G.S., 1998. A weighted Kendall's tau statistic. Statistics & probability letters 39, 17–24.

Silva, J.M., Vieira, L., Abreu, A.M., de Souza Fernandes, E., Moreira, T., da Costa, G.D., Cotta, R.M., 2023. Water, sanitation, and hygiene vulnerability in child stunting in developing countries: a systematic review with meta-analysis. Public Health 219, 117–123.

Swain, R.B., Ranganathan, S., 2021. Modeling interlinkages between sustainable development goals using network analysis. World Development 138, 105136.

United Nations, 2015. Transforming our world: the 2030 Agenda for Sustainable Development. Resolution adopted by the General Assembly on 25 September 2015 (A/RES/70/1).

Vigna, S., 2015. A weighted correlation index for rankings with ties, in: Proceedings of the 24th international conference on World Wide Web, pp. 1166–1176.

Wahid, D.F., Hassini, E., 2022. A literature review on correlation clustering: cross-disciplinary taxonomy with bibliometric analysis, in: Operations Research Forum, Springer. p. 47.

Warchold, A., Pradhan, P., Kropp, J.P., 2021. Variations in sustainable development goal interactions: Population, regional, and income disaggregation. Sustainable Development 29, 285–299.

Weitz, N., Carlsen, H., Nilsson, M., Skånberg, K., 2018. Towards systemic and contextual priority setting for implementing the 2030 agenda. Sustainability science 13, 531–548.

Wu, X., Fu, B., Wang, S., Song, S., Li, Y., Xu, Z., Wei, Y., Liu, J., 2022. Decoupling of sdgs followed by re-coupling as sustainable development progresses. Nature Sustainability 5, 452–459.

Zha, H., He, X., Ding, C., Gu, M., Simon, H., 2001. Spectral relaxation for k-means clustering. Advances in neural information processing systems 14.

Appendix A. Table of notations and definitions

Notation	Description
X^j	An indicator.
X_i	A country.
$\mathbf{x}^j = (x_i^j)$	Vector of values observed over countries for X^j.
$\mathrm{Conc}(\mathbf{x}^j, \mathbf{x}^{j'})$	Total number of concordant pairs between X^j and $X^{j'}$.
$\mathrm{Disc}(\mathbf{x}^j, \mathbf{x}^{j'})$	Total number of discordant pairs between X^j and $X^{j'}$.
$\mathrm{Tied}(\mathbf{x}^j)$	Total number of tied pairs in X^j.
$\mathbf{S}^j = (s_{ii'}^j)$	Signed matrix comparing each pair $(x_i^j, x_{i'}^j)$ for X^j.
τ_a, τ_b	Conventional Kendall coefficients.
$\mathbf{w} = (w_i)$	Vector of population sizes of countries.
τ_w	Weighted Kendall coefficient.
$\mathbb{R} = \{\mathbb{R}_l\}$	A partition of countries into regions.
$\tau_{w,\mathbb{R}}$	Within-region weighted (WRW) Kendall coefficient.
ω_l	Relative weight of region $\mathbb{R}_l$.
$\mathbf{K} = (k_{jj'})$	SDG indicators signed weighted adjacency matrix.
$\mathbf{R} = (r_{jj'})$	Binary adjacency matrix of a binary relation R.
$\mathbf{v} = (v_j)$	Eigenvector centrality measure over the indicators.
$\check{\mathbf{R}} = (\check{r}_{jj'})$	Signed adjacency matrix of a binary relation R.
$\check{\mathbf{z}} = (\check{z}_j)$	Signed vector over the indicators (encoding 2 groups).
$\tilde{\mathbf{z}} = (\tilde{z}_j)$	Real vector over the indicators.
$U, \mathbf{u} = (u_j)$	Percentage of performance, vector of values.
$V, \mathbf{v} = (v_j)$	Centrality measure, vector of values.

Table A.2: Notations and definitions used in the paper.

Appendix B. Equivalence between MRA clustering and correlation clustering

We translate the correlation clustering model introduced in (Demaine et al., 2006) into our context and using our notations. It comes:

$$\min_{\overline{\mathbf{R}} \in \{0,1\}^{\mathrm{p}\times\mathrm{p}}} \sum_{j,j'=1}^{\mathrm{p}} \Big(\widehat{P}(\mathrm{Conc}(X^j, X^{j'}))\overline{r}_{jj'} + \widehat{P}(\mathrm{Disc}(X^j, X^{j'}))(1-\overline{r}_{jj'}) \Big)$$
$$\text{s.t.} \begin{cases} \overline{r}_{jj'} = \overline{r}_{j'j}, & \forall j \neq j', \\ \overline{r}_{jj'} + \overline{r}_{j'j''} \geq \overline{r}_{jj''}, & \forall j \neq j' \neq j'', \end{cases} \tag{B.1}$$

where $\overline{\mathbf{R}} = (\overline{r}_{jj'})$ of size p × p is of general term: $\overline{r}_{jj'} = 1$ if $X^j \overline{R} X^{j'}$, that is X^j is not in relation with $X^{j'}$; $\overline{r}_{jj'} = 0$ otherwise.
Clearly $\overline{R}$ is the complement of R and $\forall j, j' : \overline{r}_{jj} = 1 - r_{jj'}$. Then, it is not difficult to see that maximizing the objective function in Problem (9) is equivalent to minimizing the objective function in Problem (B.1). Similarly, the triangular inequality constraints in Problem (B.1), $\overline{r}_{jj'} + \overline{r}_{j'j''} \geq \overline{r}_{jj''}, \forall j \neq j' \neq j''$, are identical to the transitivity inequalities in Problem (9). Thus, both 0-1 ILP models are equivalent.

Appendix C. Leading eigenvector and MRA clustering with two clusters

We demonstrate that the leading eigenvector $\mathbf{v}^1$ corresponds to the solution of a relaxed version of Problem (9), where the number of clusters is fixed at two. Our result can be seen as an extension of (Bonacich and Lloyd, 2004).

Let $\check{\mathbf{R}} = (\check{r}_{jj'})$ be a signed relational matrix associated to the binary relational matrix $\mathbf{R} = (r_{jj'})$ through the following relation, $\check{r}_{jj'} = 2r_{jj'} - 1$.

Thus, we have, $\forall j, j'$: $\check{r}_{jj'} = 1$ if $X^j R X^{j'}$; $\check{r}_{jj'} = -1$ otherwise. If R is an equivalence relation, it is not difficult to see that the characteristic properties translate into similar linear constraints as those for $\mathbf{R}$ in the case of $\check{\mathbf{R}}$: (1) reflexivity, $\forall j : \check{r}_{jj} = 1$; (2) symmetry, $\forall j \neq j' : \check{r}_{jj'} = \check{r}_{j'j}$; (3) transitivity, $\forall j \neq j' \neq j'' : \check{r}_{jj'} + \check{r}_{j'j''} - \check{r}_{jj''} \leq 1$. Moreover, we have the following relation regarding the objective function of Problem (9): $\max_{\check{\mathbf{R}} \in \{-1,1\}^{\mathrm{p} \times \mathrm{p}}} \sum_{j,j'=1}^{\mathrm{p}} k_{jj'} \check{r}_{jj'} \Leftrightarrow \max_{\mathbf{R} \in \{0,1\}^{\mathrm{p} \times \mathrm{p}}} \sum_{j,j'=1}^{\mathrm{p}} k_{jj'} (2 r_{jj'} - 1) \Leftrightarrow \max_{\mathbf{R} \in \{0,1\}^{\mathrm{p} \times \mathrm{p}}} \sum_{j,j'=1}^{\mathrm{p}} k_{jj'} r_{jj'}$. Consequently, Problem (9) is equivalent to:

$$\max_{\check{\mathbf{R}} \in \{-1,1\}^{\mathrm{p} \times \mathrm{p}}} \sum_{j,j'=1}^{\mathrm{p}} k_{jj'} \check{r}_{jj'} \text{ s.t. } \begin{cases} \check{r}_{jj} = 1, & \forall j, \\ \check{r}_{jj'} = \check{r}_{j'j}, & \forall j \neq j', \\ \check{r}_{jj'} + \check{r}_{j'j''} - \check{r}_{jj''} \leq 1, & \forall j \neq j' \neq j''. \end{cases} \tag{C.1}$$

Next, suppose that $\check{\mathbf{R}}$ encodes a partition with only two clusters. Then we can equivalently formulate $\check{\mathbf{R}}$ with respect to a vector $\check{\mathbf{z}} \in \{-1, 1\}^{\mathrm{p}}$ as follows, $\forall j, j'$: $\check{r}_{jj'} = \check{z}_j \check{z}_{j'}$, where $\check{z}_j = 1$ if X^j is in the 1st group and $\check{z}_j = -1$ if it is in the 2nd group. Note that vector $\check{\mathbf{z}} = (\check{z}_j)$ automatically implies a signed relational matrix $\check{\mathbf{R}}$ that satisfies the linear constraints of reflexivity, symmetry and transitivity in Problem (C.1). As a result, in the particular case of a partition with only two groups, we can reduce the representation of the equivalence relation from a matrix to a vector. This property makes it possible to simplify the MRA clustering model. In fact, Problem (9) with the additional constraint that $\mathbf{R}$ should encodes two clusters boils down to: $\max_{\check{\mathbf{z}} \in \{-1,1\}^{\mathrm{p}}} \check{\mathbf{z}}^\top \mathbf{K} \check{\mathbf{z}}$, where $\check{\mathbf{z}}^\top$ is the transpose of $\check{\mathbf{z}}$. This proves Lemma 1.

This discrete problem is NP-hard. In order to approximately solve it, we can replace the discrete domain $\{-1, 1\}^{\mathrm{p}}$ with the continous domain $\mathbb{R}^{\mathrm{p}}$. However, in this case, $\max_{\tilde{\mathbf{z}} \in \mathbb{R}^{\mathrm{p}}} \tilde{\mathbf{z}}^\top \mathbf{K} \tilde{\mathbf{z}}$ is not bounded since $\tilde{\mathbf{z}}$ can take

arbitrarilly high values. Therefore, denoting $\langle ., . \rangle$ the canonical dot product and $\|.\|$ the Euclidean norm in $\mathbb{R}^{\mathrm{p}}$, we additionally impose $\langle \tilde{\mathbf{z}}, \tilde{\mathbf{z}} \rangle = \|\tilde{\mathbf{z}}\|^2 = 1$ and address the following standard continuous relaxation problem $\max_{\tilde{\mathbf{z}} \in \mathbb{R}^{\mathrm{p}} : \|\tilde{\mathbf{z}}\|^2 = 1} \tilde{\mathbf{z}}^\top \mathbf{K} \tilde{\mathbf{z}}$. It is well-known that the optimal solution of this convex optimization problem is $\tilde{\mathbf{z}} = \mathbf{v}^1$, the leading eigenvector of $\mathbf{K}$. This proves Lemma 2.

Finally, combining Lemma 1 and Lemma 2 yields to Proposition 1.

Appendix D. Eigenvectors and MRA clustering with more than two clusters

In general terms, a centrality measure can be seen as a real-valued function on the vertices of a graph in order to rank them with respect to their importance in the network. In the case of a signed weighted adjacency matrix, we have shown in Subsection 3.4, that the eigenvector centrality is tightly related to the clustering of the nodes into two opposing groups.

For completeness, we show below that beyond the leading eigenvector $\mathbf{v}^1$, the subsequent eigenvectors of $\mathbf{K}$ are strongly associated with the partitionning of the vertices of the associated graph into more than two groups. Let us assume a partition of nodes into $\mathrm{k} \geq 2$ clusters denoted by $C = \{C^1, \ldots, C^{\mathrm{k}}\}$. The conventional matrix representation of such a clustering into k groups is the $\mathrm{p} \times \mathrm{k}$ binary assignment matrix $\mathbf{Z} = (z_{jl})$ of general term: $z_{jl} = 1$ if $X^j \in C^l$; $z_{jl} = 0$ otherwise.

Let us also denote $\mathbf{Z} = \begin{pmatrix} \mathbf{z}^1 & \ldots & \mathbf{z}^{\mathrm{k}} \end{pmatrix}$ where $\mathbf{z}^l = (z_{jl})_{j=1,\ldots,\mathrm{p}} \in \{0,1\}^{\mathrm{p}}$ is the binary indicator vector of cluster C^l. Let $\mathbf{e}_{\mathrm{p}}$ be the p dimensional vector with 1 in all entries. Then, the binary indicator vectors satisfy:

- Assignment to only one cluster: $\sum_{l=1}^{\mathrm{k}} \mathbf{z}^l = \mathbf{e}_{\mathrm{p}}$.

- Non-empty cluster: $\langle \mathbf{z}^l, \mathbf{e}_{\mathrm{p}} \rangle \geq 1$, for all $l = 1, \ldots, \mathrm{k}$.

It is not difficult to see that these constraints are equivalent to the following ones:

- Orthogonality: $\langle \mathbf{z}^l, \mathbf{z}^{l'} \rangle = 0$, for all $l, l' = 1, \ldots, \mathrm{k}$, such that $l \neq l'$.
- Squared Euclidean norms equal clusters sizes: $\|\mathbf{z}^l\|^2 = |C^l|$, for all $l = 1, \ldots, \mathrm{k}$.

In other words, the $\mathrm{k} \times \mathrm{k}$ matrix $\mathbf{Z}^\top \mathbf{Z} = (\langle \mathbf{z}^l, \mathbf{z}^{l'} \rangle)_{l,l'=1,\ldots,\mathrm{k}}$ is such that off-diagonal terms are null and on-diagonal entries are the cluster sizes.

In addition, we consider norming the binary indicator vectors by introducing the matrix $\breve{\mathbf{Z}} = \mathbf{Z}(\mathbf{Z}^\top \mathbf{Z})^{-1/2} = (\breve{z}_{jl})$ of general term: $\breve{z}_{jl} = \frac{1}{\sqrt{|C_l|}}$ if $X^j \in C^l$; $\breve{z}_{jl} = 0$ otherwise. In that case, the previous constraints can also be expressed in matrix notations as follows:

$$\breve{\mathbf{Z}}^\top \breve{\mathbf{Z}} = (\mathbf{Z}^\top \mathbf{Z})^{-1/2} \mathbf{Z}^\top \mathbf{Z} (\mathbf{Z}^\top \mathbf{Z})^{-1/2} = \mathbf{I}_{\mathrm{k}}, \tag{D.1}$$

where $\mathbf{I}_{\mathrm{k}}$ is the identity matrix of size $\mathrm{k} \times \mathrm{k}$.

In this paper, we have employed two ways to represent a partition: the relational matrix $\mathbf{R} \in \{0,1\}^{\mathrm{p} \times \mathrm{p}}$ and the binary assignment matrix $\mathbf{Z} \in \{0,1\}^{\mathrm{p} \times \mathrm{k}}$. In fact, we have $\mathbf{R} = \mathbf{Z}\mathbf{Z}^\top$, that is, $\forall j, j' = 1, \ldots, \mathrm{p}$: $r_{jj'} = \sum_{l=1}^{\mathrm{k}} z_{jl} z_{j'l}$. Let us express our original clustering Problem (9) with respect to $\mathbf{Z}$, assuming $\mathrm{k} \geq 2$ clusters. Firstly, observe that the objective function

of Problem (9) can be formulated as follows:

$$\begin{aligned}\sum_{j,j'=1}^{\mathrm{p}} k_{jj'} r_{jj'} = \sum_{j,j'=1}^{\mathrm{p}} k_{jj'} \sum_{l=1}^{\mathrm{k}} z_{jl} z_{j'l} = \sum_{l=1}^{\mathrm{k}} \sum_{j,j'=1}^{\mathrm{p}} k_{jj'} z_{jl} z_{j'l} &= \sum_{l=1}^{\mathrm{k}} (\mathbf{z}^l)^\top \mathbf{K} \mathbf{z}^l \\ &= \mathrm{Tr}(\mathbf{Z}^\top \mathbf{K} \mathbf{Z}) \\ &= \mathrm{Tr}(\mathbf{K} \mathbf{Z} \mathbf{Z}^\top).\end{aligned}$$

Then, by using the constraints (D.1), Problem (9) is thus equivalent to:

$$\max_{\mathbf{Z} \in \{0,1\}^{\mathrm{p} \times \mathrm{k}}} \mathrm{Tr}(\mathbf{K} \mathbf{Z} \mathbf{Z}^\top) \text{ s.t. } (\mathbf{Z}^\top \mathbf{Z})^{-1/2} \mathbf{Z}^\top \mathbf{Z} (\mathbf{Z}^\top \mathbf{Z})^{-1/2} = \mathbf{I}_{\mathbf{k}}. \tag{D.2}$$

Note that using $\breve{\mathbf{Z}}$, we have yet another equivalent formulation of Problem (9). This property relies on the the fact that $\breve{\mathbf{Z}} \breve{\mathbf{Z}}^\top = \mathbf{Z}(\mathbf{Z}^\top \mathbf{Z})^{-1} \mathbf{Z}^\top$ is an orthogonal projection matrix that should be doubly stochastic (see for example (Peng and Wei, 2007; Ah-Pine, 2022)). Therefore, Problem (9) is also equivalent to:

$$\max_{\mathbf{Z} \in \{0,1\}^{\mathrm{p} \times \mathrm{k}}} \mathrm{Tr}(\mathbf{K} \mathbf{Z} \mathbf{Z}^\top) \text{ s.t. } \mathbf{Z}(\mathbf{Z}^\top \mathbf{Z})^{-1} \mathbf{Z}^\top \mathbf{e}_{\mathrm{p}} = \mathbf{e}_{\mathrm{p}}. \tag{D.3}$$

But our focus is on the formulation stated in Problem (D.2) which remains discrete and NP-hard. As a relaxation, we can replace the discrete variable $\mathbf{Z} \in \{0,1\}^{\mathrm{p} \times \mathrm{k}}$ with the continuous variable $\tilde{\mathbf{Z}} \in \mathbb{R}^{\mathrm{p} \times \mathrm{k}}$. Furthermore, it is important to observe that the binary indicator vectors are linearly dependent since they need to satisfy $\sum_{l=1}^{\mathrm{k}} \mathbf{z}^l = \mathbf{e}_{\mathrm{p}}$. The rank of $\mathbf{Z}$ is thus $\mathrm{k}-1$ and, as a consequence, the relaxed continuous solution $\tilde{\mathbf{Z}}$ of the discrete variable $\mathbf{Z}$ should be of rank $\mathrm{k}-1$ as well. This property was implictly employed in Subsection 3.4 where the continuous relaxation of Problem (9) in the specific case of two clusters was provided by a single real variable corresponding

to the leading eigenvector.

To sum up, in the more general case $\mathrm{k} \geq 2$, the continuous relaxation of Problem (D.2) we address is the following one:

$$\max_{\tilde{\mathbf{Z}} \in \mathbb{R}^{\mathrm{p} \times (\mathrm{k}-1)}} \mathrm{Tr}(\mathbf{K}\tilde{\mathbf{Z}}\tilde{\mathbf{Z}}^\top) \text{ s.t. } \tilde{\mathbf{Z}}^\top \tilde{\mathbf{Z}} = \mathbf{I}_{\mathrm{k}-1}. \tag{D.4}$$

Likewise Subsection 3.4, Problem (D.4) has a closed-form solution. It is given by the Ky Fan theorem (Fan, 1949). In our context and using our notations, this theoretical result can be stated as follows (see also (Zha et al., 2001; Ding and He, 2004)):

Theorem 1 (Ky Fan)**.** *Let* $\mathbf{K}$ *be a* $\mathrm{p} \times \mathrm{p}$ *symmetric matrix with eigenvalues* $\lambda_1 \geq \ldots \geq \lambda_{\mathrm{p}}$ *and corresponding eigenvectors* $\mathbf{v}^1, \ldots, \mathbf{v}^{\mathrm{p}}$*. The maximization of* $\mathrm{Tr}(\mathbf{K}\tilde{\mathbf{Z}}\tilde{\mathbf{Z}}^\top)$*, where* $\tilde{\mathbf{Z}} \in \mathbb{R}^{\mathrm{p} \times (\mathrm{k}-1)}$*, subject to constraints* $\tilde{\mathbf{Z}}^\top \tilde{\mathbf{Z}} = \mathbf{I}_{\mathrm{k}-1}$*, has the solution* $\tilde{\mathbf{Z}} = \mathbf{V}^{\mathrm{k}-1}\mathbf{S}$*, where* $\mathbf{V}^{\mathrm{k}-1} = \begin{pmatrix} \mathbf{v}^1 & \ldots & \mathbf{v}^{\mathrm{k}-1} \end{pmatrix} \in \mathbb{R}^{\mathrm{p} \times (\mathrm{k}-1)}$ *and* $\mathbf{S} \in \mathbb{R}^{(\mathrm{k}-1) \times (\mathrm{k}-1)}$ *is an arbitary orthonormal matrix. Furthermore we have* $\max \mathrm{Tr}(\mathbf{K}\tilde{\mathbf{Z}}\tilde{\mathbf{Z}}^\top) = \lambda_1 + \ldots + \lambda_{\mathrm{k}-1}$.

In (Zha et al., 2001; Ding and He, 2004), the authors introduce diverse approaches to recover a discrete (approximate) solution $\mathbf{Z}$ from the continuous relaxed outcome $\tilde{\mathbf{Z}}$. They either reason with the orthogonal matrix $\mathbf{S}$ or with the following matrix $\tilde{\mathbf{Z}}\tilde{\mathbf{Z}}^\top = \mathbf{V}^{\mathrm{k}-1}\mathbf{S}\mathbf{S}^\top(\mathbf{V}^{\mathrm{k}-1})^\top = \mathbf{V}^{\mathrm{k}-1}(\mathbf{V}^{\mathrm{k}-1})^\top$.

We have exposed the relationships between the MRA clustering framework and the eigendecomposition of the signed weighted adjacency matrix $\mathbf{K}$ in the general case with $\mathrm{k} \geq 2$ clusters. This demonstrates from a broad viewpoint, the consistency of our network analysis framework that integrates MRA clustering with eigencentrality. However, in this paper, we do not exploit the full spectrum but restrict ourselves to the first leading eigenvector

only as explained at the end of Subsection 3.4.

Appendix E. SDR 2024 Dataset and percentages of performance

For any numerical indicator X^j, we assume two thresholds: w^j and b^j, representing the worst- and best-case scenarios. Depending on the indicator, these may correspond to upper and lower bounds, or *vice versa*. For example, for X^j = sdg3_neonat (Neonatal mortality rate), the worst case is at the upper bound ($w^j = 40/1000$) and the best at the lower bound ($b^j = 1.1/1000$). Conversely, $X^{j'}$ = sdg3_births (Births attended by skilled health personnel) has its worst case at the lower bound ($w^{j'} = 23\%$) and best at the upper bound ($b^{j'} = 100\%$).

The initial value of indicator X^j for country X_i, denoted d_i^j, is converted into a percentage of achievement x_i^j using the transformation defined in (Sachs et al., 2024; Lafortune et al., 2018): (1) first, the data distributions across countries are censored, meaning that any value d_i^j falling outside the interval $[\min(w^j, b^j), \max(w^j, b^j)]$ is set to the nearest bound; (2) next, the data are normalized to obtain a percentage of performance x_i^j that increases with proximity to the best-case scenario. For all indicators, higher values of x_i^j (closer to 100%) indicate better performance and greater progress toward achieving the target associated with indicator X^j. This normalization is given by, $\forall j = 1, \ldots, \mathrm{p}$ and $\forall i = 1, \ldots, \mathrm{n}$:

$$x_i^j = \frac{|d_i^j - w^j|}{|b^j - w^j|} 100. \tag{E.1}$$

Appendix F. Numerical details on MRA clustering 0-1 ILP

All procedures were implemented in Python and executed on an HP EliteBook laptop with an Intel Core i5-1335U processor, 16 GB of RAM,

running Ubuntu 22.04.

In order to solve the MRA clustering Problem (9), we used the open-source PuLP library (Mitchell et al., 2011) and CBC MIP solver (Forrest and Lougee-Heimer, 2005).

We provide some numerical performances in Table F.3. The row referred to as "Global" corresponds to the optimal partition we obtained at the global scale and discussed previously in Section 4.2. The remaining rows present additional results corresponding to the partitionning of the SDG networks of the 96 indicators assessed in each region using the weighted Kendall coefficient. The related structured chord diagrams are given in the supplementary materials.

Case	Nb. of clusters	Objective value	Time (CPU seconds)
Global	2	2105.25	253.29
Eastern Europe & Central Asia	3	1567.39	1051.29
East & South Asia	3	2479.19	279.25
Latin America and the Caribbean	3	1564.95	3932.47
Middle East and North Africa	3	1196.64	1020.56
OECD members	3	1523.94	1906.58
Sub-Saharan Africa	3	871.74	3779.54

Table F.3: Numerical results for computing the MRA optimal clustering.

Appendix G. Tables of WRW Kendall correlations and criteria U and V values for Pareto-Clusters

Acronym	**sdg6_wastewat**	**sdg14_cpma**	**sdg9_rdex**	**sdg16_cpi**	**sdg9_articles**	**sdg16_admin**	**sdg3_uhc**	**sdg2_stunting**	**sdg11_slums**	sdg7_renewcon	sdg16_exprop	sdg12_pollprod	sdg12_ewaste
sdg6_wastewat	1.00	0.12	0.13	0.22	0.16	0.22	0.20	0.20	0.18	0.00	0.22	-0.05	-0.13
sdg14_cpma	0.12	1.00	-0.12	-0.05	-0.08	0.08	0.01	0.23	0.20	-0.45	-0.27	0.17	-0.10
sdg9_rdex	0.13	-0.12	1.00	0.72	0.74	0.58	0.78	0.47	0.55	-0.10	-0.23	-0.67	-0.58
sdg16_cpi	0.22	-0.05	0.72	1.00	0.79	0.68	0.76	0.50	0.59	-0.08	-0.14	-0.65	-0.58
sdg9_articles	0.16	-0.08	0.74	0.79	1.00	0.60	0.78	0.55	0.61	-0.12	-0.28	-0.69	-0.64
sdg16_admin	0.22	0.08	0.58	0.68	0.60	1.00	0.66	0.66	0.63	-0.27	-0.33	-0.47	-0.64
sdg3_uhc	0.20	0.01	0.78	0.76	0.78	0.66	1.00	0.56	0.64	-0.04	-0.21	-0.60	-0.65
sdg2_stunting	0.20	0.23	0.47	0.50	0.55	0.66	0.56	1.00	0.69	-0.31	-0.48	-0.43	-0.62
sdg11_slums	0.18	0.20	0.55	0.59	0.61	0.63	0.64	0.69	1.00	-0.17	-0.37	-0.41	-0.77
sdg7_renewcon	0.00	-0.45	-0.10	-0.08	-0.12	-0.27	-0.04	-0.31	-0.17	1.00	0.43	0.02	0.23
sdg16_exprop	0.22	-0.27	-0.23	-0.14	-0.28	-0.33	-0.21	-0.48	-0.37	0.43	1.00	0.24	0.37
sdg12_pollprod	-0.05	0.17	-0.67	-0.65	-0.69	-0.47	-0.60	-0.43	-0.41	0.02	0.24	1.00	0.44
sdg12_ewaste	-0.13	-0.10	-0.58	-0.58	-0.64	-0.64	-0.65	-0.62	-0.77	0.23	0.37	0.44	1.00

Table G.4: WRW Kendall correlation network of indicators in the Pareto front of each cluster. Pareto-Cluster 1 is in **bold**.

Acronym	Description	U	V
sdg6_wastewat	Anthropogenic wastewater that receives treatment (%)	13.13	0.024
sdg14_cpma	Mean area that is protected in marine sites important to biodiversity (%)	30.36	0.041
sdg9_rdex	Expenditure on research and development (% of GDP)	31.27	0.114
sdg16_cpi	Corruption Perceptions Index (worst 0-100 best)	35.76	0.117
sdg9_articles	Articles published in academic journals (per 1,000 population)	37.22	0.121
sdg16_admin	Timeliness of administrative proceedings (worst 0 - 1 best)	46.01	0.123
sdg3_uhc	Universal health coverage (UHC) index of service coverage (worst 0-100 best)	47.39	0.124
sdg2_stunting	Prevalence of stunting in children under 5 years of age (%)	52.17	0.129
sdg11_slums	Proportion of urban population living in slums (%)	70.17	0.133
sdg7_renewcon	Renewable energy share in total final energy consumption (%)	20.07	-0.055
sdg16_exprop	Expropriations are lawful and adequately compensated (worst 0 - 1 best)	27.34	-0.087
sdg12_pollprod	Production-based air pollution (DALYs per 1,000 population)	57.64	-0.095
sdg12_ewaste	Electronic waste (kg/capita)	70.86	-0.130

Table G.5: Acronyms, descriptions, weighted means of percentages of performance (U), and eigencentrality scores (V) for indicators in the Pareto front of each cluster. Pareto-Cluster 1 is in **bold**.